Coherent elastic and rotationally inelastic scattering of N_2, O_2, and CH_4 from a 10 K Cu(111) surface

T. Andersson, F. Althoff, P. Linde, M. Hassel, M. Persson,[a] and S. Andersson
Department of Applied Physics, Chalmers University of Technology and Göteborg University, SE-412 96 Göteborg, Sweden

(Received 14 July 2000; accepted 29 August 2000)

We report observations of coherent elastic and rotationally inelastic scattering of N_2, O_2, and CH_4 from a 10 K Cu(111) surface, kept clean by pulsed laser heating. The related sharp features in the measured angular distributions decrease drastically in intensity at elevated target temperatures. At low temperature rotational transitions reduce the elastic scattering probability by about an order of magnitude. This effect is weak for D_2 at the impact conditions of concern. Quantum scattering calculations for N_2 and D_2 show that this difference is primarily caused by the large difference in rotational constants and the associated rotational transition energies of these molecules. © *2000 American Institute of Physics.* [S0021-9606(00)70344-8]

I. INTRODUCTION

Coherent quantum scattering of molecules from solid surfaces is usually associated with light particles like hydrogen and its isotopic variants. Early experiments using hydrogen molecular beams established important physical phenomena in molecule–surface collisions like diffraction, selective adsorption and rotationally inelastic diffraction. Nowadays, such measurements allow, in the case of physical adsorption, precise and detailed determination of the molecule–surface interaction potential. Even fine details like the orientational dependence can be measured using hydrogen beams of different composition with respect to even and odd rotational states.

Diffraction of the weakly bound hydrogen dimer has been reported[1] but otherwise observations of coherent quantum scattering events involving heavier diatomic and polyatomic molecules are in general lacking and seem difficult to obtain. The probability for such events to occur is, for example, profoundly influenced by the target temperature. A slow heavy molecule will exert a slowly varying force on the surface atoms and hence predominantly interact with the low-frequency lattice vibrations whose populations are most sensitive to a low surface temperature.[2,3] At elevated temperatures the lattice thermal motion will, via the Debye–Waller factor, e^{-2W}, drastically reduce all coherent elastic and inelastic scattering probabilities. In general, heavier molecules also experience deeper physisorption wells and consequently interact more strongly with the lattice vibrations, further increasing the influence of the lattice thermal motion on the scattering pattern.

The elastic scattering probabilities of low-energy H_2 and D_2 beams from a cold inert metal surface are substantial and only weakly affected by rotational excitations.[4] This is a consequence of the large rotational excitation energies, the $j=0\rightarrow 2$ transition occurs at 44 and 22 meV for H_2 and D_2, respectively, and the weak anisotropic forces associated with the almost spherical molecular charge distribution. D_2 and N_2 have equivalent rotational spectra (2/3 and 1/3 of the molecules in even j and odd j states, respectively) but N_2 has a much smaller rotational constant (larger moment of inertia) than D_2, the $j=0\rightarrow 2$ transition energy is around 1.5 meV. One may intuitively argue that rotational transitions should, for this reason alone, influence the elastic scattering probability much more for N_2 than for D_2.

In this paper we report observations of coherent elastic and rotationally inelastic scattering of D_2, N_2, O_2, and CH_4 molecular beams from a cold Cu(111) surface. The different coherent scattering events have been analyzed by varying the scattering angle and the substrate temperature. In particular, we have disentangled the effects of rotational and phonon inelasticity on the elastic scattering. The role of the rotational energy spacing and the orientational anisotropy of the molecule–surface interaction on the rotational inelasticity has been studied for D_2 and N_2 using quantum scattering calculations with potential energy surfaces, which are partly based on density functional calculations. The calculations show that the relative magnitude of the rotational energies to the kinetic energy at the potential energy minimum has a dramatic influence on the rotational excitation probability.

II. EXPERIMENT

For the impact conditions of our experiment, N_2, O_2, and CH_4 physisorb on the cold Cu(111) surface and desorb at temperatures in the range 35–50 K. As an atomic reference beam we have used Ar, which desorbs just below 40 K. Below these temperatures, beam particles stick and accumulate on the surface and the coherent scattering pattern is, as a consequence, rapidly obliterated. Desorbing the stuck particles by pulsed laser heating turns out to provide a simple method to overcome this problem, at least for N_2, CH_4, and Ar.[5] For this purpose we have used a Lambda Physik XeCl excimer laser operating at a laser power <3 MW/cm^2 and 20 ns pulse duration. A repetition rate around a few hertz is in general sufficient to keep the surface clean, while the

[a]Electronic mail: tfymp@fy.chalmers.se

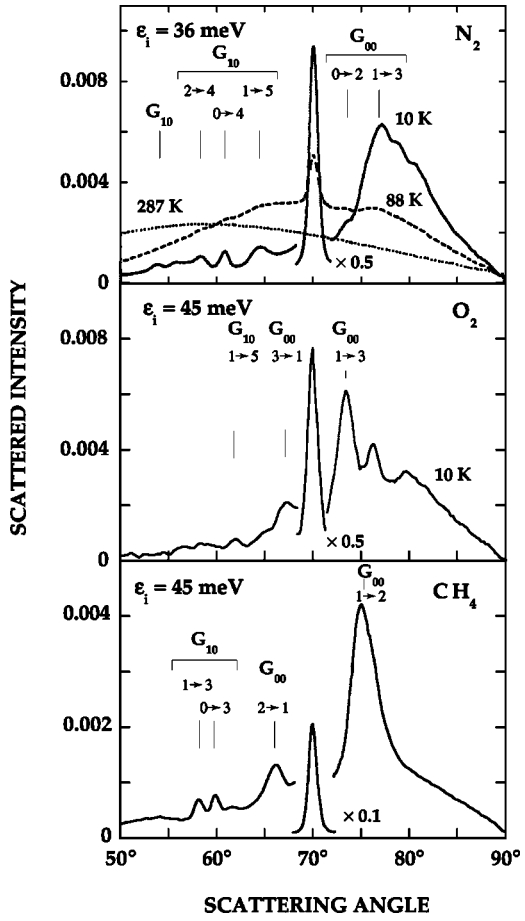

FIG. 1. Measured angular distributions of N_2, O_2, and CH_4 scattered from Cu(111) at different surface temperatures. The energy of the incident beam is 36 (45) meV for N_2 (O_2, CH_4) and the angle of incidence is 70° from the surface normal.

mean surface temperature is almost unaffected. We have used specular elastic He scattering measurements to monitor possible laser-induced surface damage.[6] At the modest desorption temperatures required in our low-temperature scattering measurements such damage presents no disturbance.[7]

The scattering experiments discussed here were performed in a cryopumped ultrahigh vacuum chamber operating in the low 10^{-11} Torr range and attached to a differentially pumped nozzle beam source. Incident and scattered beam intensities were measured using a rotatable stagnation detector with an angular resolution of 0.8°. The angular divergence of the incident beam is around 0.1°. The low-energy molecular beams (N_2, O_2, CH_4) are rotationally cold; the rotational temperature is around 15 K. The Cu(111) specimen was oriented so that at off-normal incidence, the scattering plane defined by the incident and specular particle beams comprised the surface normal and the [112] direction in the surface plane. The x-ray aligned ($<0.2°$) and polished specimen was cleaned *in situ* by standard methods involving argon-ion bombardment and heating cycles. Further details concerning the apparatus, the specimen preparation, and the experimental procedure are presented elsewhere.[4]

Angular distributions of N_2, O_2, and CH_4 beams scattered from a Cu(111) surface kept at 10 K are shown in Fig. 1. The distributions were measured in the scattering plane for

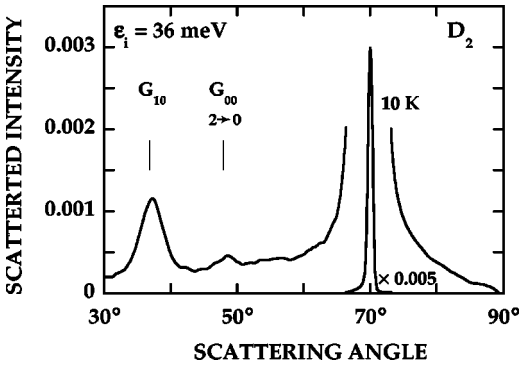

FIG. 2. Measured angular distribution for D_2 scattered from a 10 K Cu(111) surface. Incidence conditions are as in Fig. 1.

an angle of incidence $\theta_i = 70°$ from the surface normal and beam energies of 36 meV for N_2 and 45 meV for O_2 and CH_4, respectively. Data for N_2 obtained at three target temperatures (see the top panel) reveal that pronounced sharp features in the angular scans are observed only at a low temperature. The features comprise elastic and inelastic scattering events like an intense specular elastic peak at 70° and various peaks involving rotational transitions of the molecules during the interaction with the surface. In the angular range 30°–70°, the peaks follow the kinematic conditions for diffraction and rotationally inelastic diffraction associated with surface reciprocal lattice vectors $\boldsymbol{G}_{hk}$ and with rotational transitions $j \rightarrow j'$ of energy $\epsilon_{jj'}$, $\epsilon_s = \epsilon_i - \epsilon_{jj'}$ and $\boldsymbol{K}_s = \boldsymbol{K}_i + \boldsymbol{G}_{hk}$. Here ϵ_i, ϵ_s, $\boldsymbol{K}_i$, and $\boldsymbol{K}_s$ refer to the energies and the wave-vector components parallel to the surface of the incident and scattered beams. We have labeled prominent peaks by the relevant $\boldsymbol{G}_{hk}$ and $j \rightarrow j'$ indices.[8] The first-order elastic diffraction peaks, (10), are in general quite weak and most of the diffraction intensity appears in the rotationally inelastic diffraction peaks. In the case of H_2 and D_2 scattering, the situation is in general the reverse, that is, the rotationally inelastic diffraction peaks are weaker than the elastic diffraction peaks.[9] An angular scan, shown in Fig. 2, for D_2 scattered from Cu(111) at 10 K illustrates this point (incidence conditions as for N_2).

The angular scans are more complex in the range 70°–90°, in particular for N_2 and O_2. While the CH_4 data reveal a distinct ($\boldsymbol{G}_{00}$,1→2) peak around 75°, the N_2 and O_2 scans show several sharp peaks superimposed on a broad phonon emission peak. The latter situation is clearly illustrated in Fig. 3, which presents a comparison between the angular distributions for N_2 and Ar. The broad, smooth peak centered around 77° in the Ar scan originates from phonon emission processes, while the intensity of the complementary phonon absorption processes at scattering angles $\theta_s < 70°$ is strongly suppressed at the low target temperature of concern. The peaks superimposed on the broad phonon emission peak for N_2 (and O_2) are not related to rotational transitions in the simple manner discussed previously. This is illustrated in Fig. 4, which displays the measured peak positions, θ_s vs ϵ_i, together with the kinematical conditions for relevant rotational transitions. The peak closest to the specular one, in the range 70°–90°, follows reasonably well the dispersion of a $\boldsymbol{G}_{00}$,0→2 event for N_2 ($\boldsymbol{G}_{00}$,1→3 for O_2) while the other

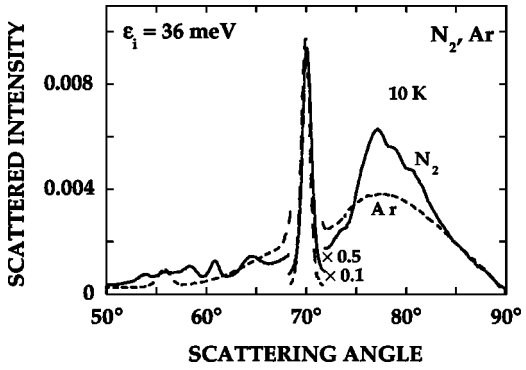

FIG. 3. Comparison of measured angular distributions of Ar and N_2 scattered from a 10 K Cu(111) surface. Incidence conditions are as in Fig. 1.

features in this range have no such simple interpretation. The most likely explanation is that these peaks involve simultaneous rotational transition and phonon emission.[10,11]

The sharp details of the angular distributions shown in Fig. 1 decrease drastically in intensity when the target temperature is increased. As shown for N_2 in Fig. 1, only a weak specular elastic peak superimposed on a broad inelastic distribution remains at 88 K. Diffraction peaks are weak relative to the specular peak in the angular distributions and we can regard the specular elastic peak as a good measure of the elastically scattered fraction. We will consider the temperature dependence of the elastic scattering in more detail starting from the data shown in Fig. 5, where in the top panel we have plotted the normalized specular reflectivity for D_2 and N_2, as $\ln I_{00}$ versus target temperature, T. Data are plotted for different values of the initial translational energy, $\epsilon_\perp = \epsilon_i \cos^2 \theta_i$, perpendicular to the surface, with incidence conditions given by $\epsilon_i = 36$ meV and $\theta_i = 70°$ for $\epsilon_\perp = 4.2$ meV (N_2 and D_2), $\epsilon_i = 36$ meV and $\theta_i = 60°$ for $\epsilon_\perp = 9.0$ meV (N_2), and $\epsilon_i = 112$ meV and $\theta_i = 45°$ for $\epsilon_\perp = 56$ meV (D_2). The lower panel shows data for O_2, CH_4, and Ar. Incidence conditions are $\epsilon_\perp = 4.2$ meV ($\epsilon_i = 36$ meV and $\theta_i = 70°$) for O_2 and Ar and $\epsilon_\perp = 4.8$ meV ($\epsilon_i = 41$ meV and $\theta_i = 70°$) for CH_4. Data for Ar have been included for comparison since the inelastic scattering in this case only involves phonon processes and hence the data represent a good measure of the elastically scattered fraction given by the Debye–Waller factor e^{-2W}. If we for Ar, as shown in Fig. 5, extrapolate the linear decay, $2W = \beta T$, of $\ln I_{00}$ observed at higher temperatures, to $T = 0$ K, we obtain a value of $\ln I_{00}$ around -0.1 rather than 0, which we would expect for a rigid lattice in the case of weak diffraction. We believe that this deviation derives from diffuse elastic scattering due to surface imperfections. The linear decay of $\ln I_{00}$ with T for D_2 also extrapolates to a value of $\ln I_{00}$ around -0.1 at $T = 0$ K.

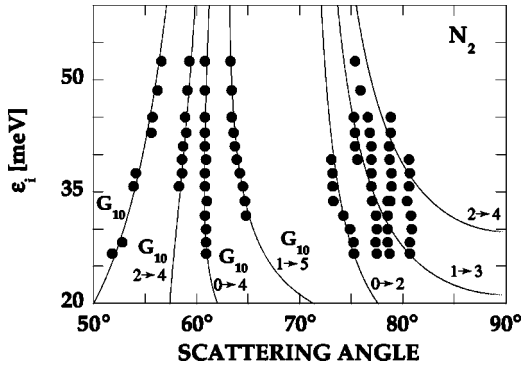

FIG. 4. Angular positions of peaks in the N_2 scan at different incident energies, ϵ_i. The solid curves are kinematical free particle dispersion relations for rotational inelastic diffraction events.

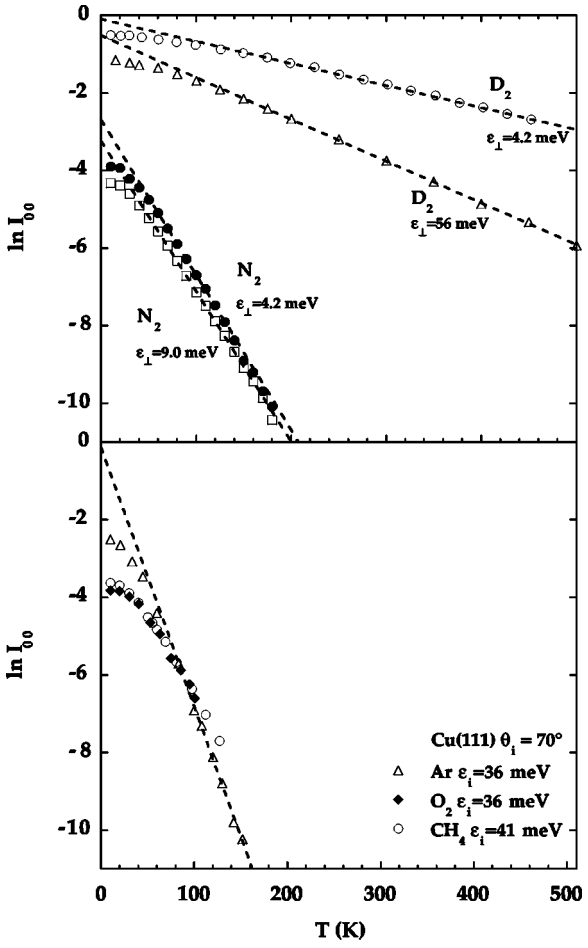

FIG. 5. Normalized specular reflectivity, I_{00}, plotted as $\ln I_{00}$ vs target temperature. The upper panel shows data for D_2 and N_2 obtained for a beam energy of 36 meV, with angles of incidence $\theta_i = 70°$ and $\theta_i = 60°$ for $\epsilon_\perp = 4.2$ meV and $\epsilon_\perp = 9.0$ meV, respectively. Data for D_2 measured at 45° and 112 meV are included for comparison. The lower panel shows data for Ar, O_2, and CH_4 obtained at 70° and 36 meV (41 meV for CH_4).

The data for N_2, O_2, and CH_4 behave in a different manner. Extrapolating the linear decay for N_2 at $\epsilon_\perp = 4.2$ meV to $T = 0$ K gives a value of $\ln I_{00}$ around -2.9 rather than a small value -0.1 as we found for Ar. The corresponding values -2.5 and -2.3 for O_2 and CH_4, respectively, are also large. This difference we attribute to rotational transitions, which introduce new inelastic scattering channels for the molecules and reduce the specular scattering of N_2, for example, by more than an order of magnitude at our impact conditions. At the same incidence conditions ($\epsilon_\perp = 4.2$ meV) D_2 behaves just like Ar, which implies that rotational transitions are rather unimportant for this molecule at these incidence conditions. Data for D_2 obtained at $\epsilon_\perp = 56$ meV (see Fig. 5) show a different behavior, however. In this case the

normal energy $\epsilon_\perp$ is substantially larger than the $j=0\rightarrow 2$ rotational excitation energy around 22 meV. Extrapolating the linear decay to $T=0$ K gives a value of $\ln I_{00}$ around -0.5 while for Ne, for example, at similar incidence conditions a small value of -0.1 is observed. The specular elastic reflectivity of D_2 is hence reduced by about 30% in this case, most likely due to rotational transitions. When evaluating the D_2 data we note that the D_2 beam is not rotationally cold in the same way as the N_2 beam.[12] We estimate the rotational temperature to be around 100 K ($\epsilon_i=36$ meV) and 300 K ($\epsilon_i=112$ meV), respectively.

N_2 has just like D_2 a rotational energy spectrum, $E=Bj(j+1)$, with 2/3 of the molecules in even j states (*ortho*) and 1/3 in odd j states (*para*) but with widely different rotational constants; $B=0.248$ and 3.70 meV for N_2 and D_2, respectively. One may intuitively argue that rotational transitions should influence the elastic scattering probability much more profoundly for N_2 than for D_2 because of the small rotational transition energies of N_2. Other factors like the potential well-depth and orientational anisotropy of the molecule–surface interaction potential also contribute and we will give a detailed discussion of the relative importance of rotational transitions for these molecules in relation to the quantum scattering calculations presented in the following.

The plots in Fig. 5 also give information about the interaction of the particles with the phonons of the solid lattice. Toward lower temperatures all the data in Fig. 5 deviate from a linear behavior and eventually level off at approximately temperature independent values. At 10 K and $\epsilon_\perp=4.2$ meV, $\ln I_{00}=-4.0$ and -3.8 for N_2 and O_2, respectively, and we can obtain an estimate of the low-temperature Debye–Waller exponent for these molecules by subtracting the contribution due to rotational transitions, which gives $2W=4.0-2.9=1.1$ for N_2 and $2W=3.8-2.5=1.3$ for O_2. Experimental observations for Ar and Kr[13] are consistent with predictions from semiclassical theory,[2,3] which state that the probability for elastic scattering of heavy atoms is independent of particle mass at low surface temperature and depends on the square root of the mass at elevated temperatures. The elastic scattering depends sensitively on the well depth of the gas–surface interaction potential and the impact parameters. The potential well depths for N_2, O_2, and Ar ought to be rather similar since they desorb at almost equal temperatures. We would then expect the low-temperature value of $2W$ for N_2 and O_2 to be close to the value of $2W=2.23$ for Ar, if the molecules interact with the lattice vibrations in the same way as the heavier inert gases at low surface temperature. Our estimated values of 1.1 and 1.3 are clearly smaller and the phonon inelastic scattering for diatomic molecules like N_2 and O_2 is evidently substantially weaker than for a corresponding inert gas atom. This effect is well established in gas–surface scattering and derives from translation–rotation energy transfer, which cushions the impact and consequently weakens the particle–phonon interaction.[14] The cushioning effect of this energy transfer also reduces the slope of $\ln I_{00}$ observed at higher temperatures. The measured values of β, in the linear region, $2W=\beta T$, are 0.038 and 0.067 for N_2 and Ar, respectively. From the previous discussion we would expect the β values to scale as $m^{1/2}$, where m is the particle mass. The measured value for N_2 is clearly smaller than the value $\beta=[28/40]^{1/2}\times 0.067=0.056$ we estimate from an $m^{1/2}$ scaling of β for Ar. This observation is consistent with the weakened N_2–phonon interaction due to translation–rotation energy transfer.

III. THEORY

To scrutinize our intuitive picture of the behavior of rotational transitions and their influence on the elastic scattering intensity for various molecules, we have calculated probabilities for rotational transitions of N_2 and D_2 scattering from a cold Cu(111) surface. The calculations are based on a numerical wave-packet propagation on a rigid two-dimensional model potential energy surface (PES), which depends on the distance, z, between the molecule and the surface, and on the angle, θ, between the molecular axis and the surface normal. The rotational transitions of the molecule are then governed by the orientational anisotropy of the PES, that is, the dependence of the potential on θ, and the moment of inertia. By monitoring the rotational distribution of the time-evolving wave packet, we obtain the probabilities for rotational transitions during the scattering event.

At the low translational energies of concern here, the molecules experience physisorption interaction with the surface. We have used the current theoretical description of molecular physisorption,[15] with the laterally and rotationally averaged interaction, $V_0(z)$, described by a superposition of a Pauli repulsive branch and a van der Waals attractive branch given by

$$V_R(z)=C_R e^{-\alpha z}, \tag{1}$$

and

$$V_{\mathrm{vdW}}(z)=-C_{\mathrm{vdW}}\frac{f(2k_c(z-z_{\mathrm{vdW}}))}{(z-z_{\mathrm{vdW}})^3}, \tag{2}$$

respectively. Here C_R describes the strength and $1/\alpha$ describes the range of the repulsive interaction, z_{vdW} is the position of the van der Waals reference plane. For D_2–Cu(111), $V_0(z)$ is well characterized from previous work.[15] For N_2–Cu(111), we have used parameters derived for Ar–Cu(111),[16] since thermal desorption experiments suggest similar well depths in these cases. The anisotropy of the potential was described, in a conventional manner, by the lowest order term in an expansion in Legendre polynomials,

$$V(z,\theta)=V_0(z)+V_2(z)P_2(\cos(\theta)), \tag{3}$$

where the anisotropic term is written as a linear combination of $V_R(z)$ and $V_{\mathrm{vdW}}(z)$,

$$V_2(z)=\beta_R V_R(z)+\beta_{\mathrm{vdW}}V_{\mathrm{vdW}}(z). \tag{4}$$

The coefficient β_{vdW} was determined from the static polarizability of the molecule,[17] while β_R was determined from total energy, density functional theory calculations.[18] We find that the resulting rotational splittings of the bound levels of H_2 in the D_2–Cu potential are in good agreement with

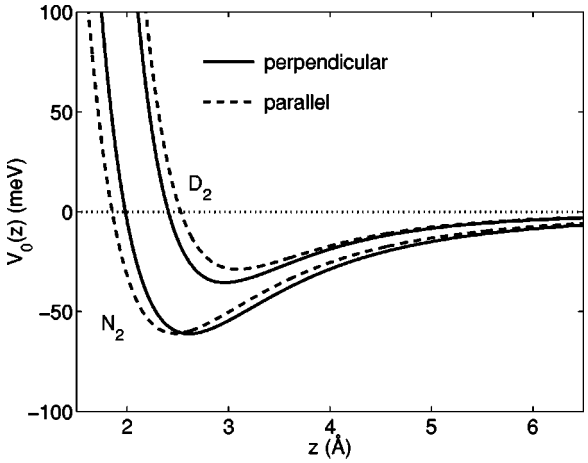

FIG. 6. Model potential energy surfaces for D_2 and N_2 on Cu(111). The solid and dashed lines correspond to molecules perpendicular and parallel to the surface, respectively. For D_2, the z axis has been offset by 1 Å for clarity.

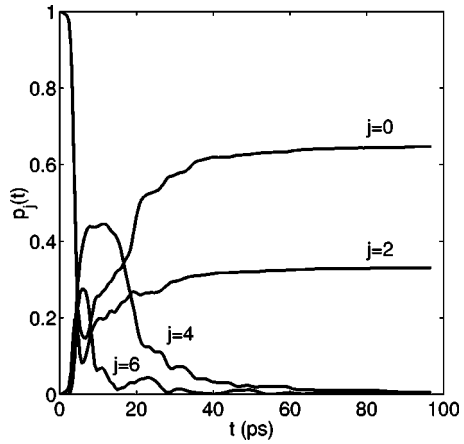

FIG. 7. Calculated rotational probability distribution, $p_j(t)$, for scattering of N_2 from a Cu(111) surface. Initially, the molecule is in the $j=0$ state with a normal translational energy of $\epsilon_\perp = 4.2$ meV.

experimental data for H_2 on Cu(100).[19] This agreement gives us confidence in our approach for determining the rotational anisotropy.

In Fig. 6, we show our resulting potentials for molecules oriented perpendicular and parallel to the surface. Note that the anisotropy for D_2 favors a perpendicular orientation of the molecule, which is consistent with results from a previous study of $H_2-Cu(100)$.[19] Otherwise, we find that the orientational anisotropies of the PESs for D_2 and N_2 are similar in magnitude.

The rotational distribution of the molecule scattering from the surface was determined by the time evolution of a wave packet using a pseudospectral method. This method is based on a discrete variable representation[20] of the Schrödinger equation with periodic boundary conditions in the z direction and the split-operator approximation for the short-time propagator. To prevent the scattered wave from interacting with the backside of the repulsive potential barrier, we have introduced an absorbing potential[21] at the grid boundary. The initial wave function was represented by a Gaussian function in the z coordinate, with an energy uncertainty of 10%, and a definite rotational state in the θ coordinate. The probability, $p_j(t)$, to find the molecule in a rotational state j was calculated by projecting the wave packet, at each time step, onto the rotational eigenstates of the free rotor.

In Fig. 7, we show our results for the rotational probability distributions for scattering of a N_2 molecule with an initial translational energy $\epsilon_\perp = 4.2$ meV perpendicular to the surface and rotational state $j=0$. Evidently, there is a maximum of 85% probability for rotational excitation when the molecule is located in the region of the physisorption well and the dominant part of $p_j(t)$ is in the $j=4$ state. After several tens of picoseconds the molecule leaves the physisorption well and the rotational energy is transferred back to the translational coordinate, resulting in a final state with a probability of about 35% in rotationally excited states. Note that for $j \geqslant 4$ states the rotational energy is larger than the incident energy, so these states are trapped in the potential well and are closed channels. For a higher incident energy, $\epsilon_\perp = 9.0$ meV, the maximum probability for rotational excitation increases, slightly, to 89%.

Our results for a rotationally cold D_2 ($j=0$), with two different initial translational energies, $\epsilon_\perp = 4.2$ and 56 meV, are shown in Fig. 8. For the lower energy, there is at most only a 2% probability for rotational excitations to $j=2$. No real excitations to $j=4$ can occur energetically. The $j=2$ state is a closed channel and is trapped in the potential well, because the rotational energy, 22 meV, for $j=0 \rightarrow 2$ is much larger than the initial energy. For the higher initial energy of 56 meV, there is about 22% probability for excitation to the $j=2$ state, which in this case has enough translational energy to traverse the potential well.

The calculations show that the larger rotational excitation probability for N_2 than for D_2 is not caused by differences in the rotational anisotropy of the respective PES. This point is demonstrated by the results for the rotational distribution for D_2 in the model PES for N_2 at an incidence energy of 4.2 meV and rotational state of $j=0$. In this situation we find that the calculated maximum rotational excitation probability is about 15%, which is much less than the correspond-

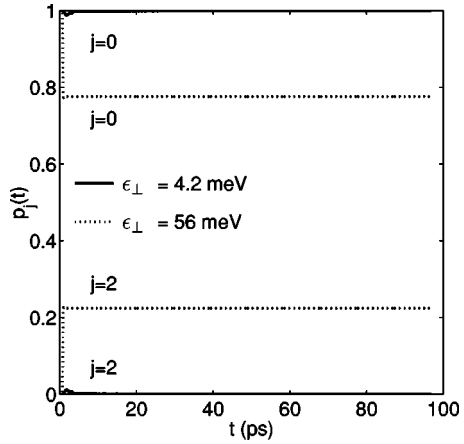

FIG. 8. Calculated rotational probability distribution, $p_j(t)$, for scattering of D_2 from a Cu(111) surface. Initially, the molecule is in the $j=0$ state and the solid and dotted lines correspond to a molecule with initial translational energy of 4.2 and 56 meV, respectively.

ing probability of about 85% for N_2. Thus the large difference in rotational excitation probabilities between D_2 and N_2 is instead caused by the large difference in the moments of inertia. This result also illustrates the effect that the relative magnitude of the rotational energies, compared to the kinetic energy at the potential energy minimum, has a dramatic influence on the rotational excitation probability. For D_2 in the H_2 potential, the rotational energies are comparable to the kinetic energy gain in the potential well resulting in a small rotational excitation probability of about 2% compared to the corresponding probability of about 15% for scattering in the PES of N_2, for which the potential well is about twice as deep.

IV. COMPARISON BETWEEN THEORY AND EXPERIMENTS

The results from our calculations are consistent with the experimentally observed elastic intensities. To make a direct comparison with experiments, we have made an average of $p_j(0)$ over the initial distribution of various j set by the rotational temperature T_{rot} of the incident molecular beam and its normal distribution of *para* and *ortho* molecular states. For N_2 at $\epsilon_\perp = 4.2$ meV and $T_{\mathrm{rot}} = 15$ K, the calculations show a 80% probability for rotational transitions, compared with the measured elastic intensity that was reduced by about 95% due to such excitations. Although in the calculations, the rotationally excited, trapped states eventually transform their energy back to the translational coordinate, leading to the elastic intensity being reduced by only 45%, we believe that in a more realistic model including phonon excitations, the rotational energy acquired in the physisorption well is mainly lost irreversibly to the substrate.[22] For D_2, on the other hand, the calculated probability for rotational transitions is, at $\epsilon_\perp = 4.2$ meV and $T_{\mathrm{rot}} = 100$ K, negligible during the roundtrip in the well in agreement with the experimental observations. At larger energy $\epsilon_\perp = 56$ meV and $T_{\mathrm{rot}} = 300$ K, the probability for rotational transitions becomes substantial. We find that the calculated probability, around 17% for these events, compares reasonably well with the probability of 30% estimated from the reduction of the measured elastic intensity.

V. SUMMARY

Using pulsed laser heating to prevent stuck particles from accumulating on the cold surface, we have shown that coherent elastic and rotationally inelastic scattering of heavy molecules such as N_2, O_2, and CH_4 from a 10 K Cu(111) surface can be observed. Rotational transitions were found to reduce the elastic as well as the phonon inelastic scattering. The sharp coherent rotation features in the measured angular distributions decrease in intensity with increasing target temperature. At low temperatures, rotational transitions reduce the elastic scattering probability for N_2 by about an order of magnitude. This effect is weak for D_2 at the impact conditions of concern. Quantum scattering calculations, using realistic potential energy surfaces for N_2 and D_2, have revealed that this difference is primarily caused by the large difference in rotational constants and the associated rotational transition energies of these molecules.

ACKNOWLEDGMENTS

Financial support from the Swedish Research Councils for Natural Science (NFR) and Engineering Sciences (TFR) is gratefully acknowledged. We are also grateful for computer resources provided by the center for parallel computers (PDC) in Stockholm.

[1] G. Tepper and D. Miller, Phys. Rev. Lett. **69**, 2927 (1992).
[2] A. C. Levi and H. Suhl, Surf. Sci. **88**, 221 (1979).
[3] K. Burke and W. Kohn, Phys. Rev. B **43**, 2477 (1991).
[4] S. Andersson, L. Wilzén, M. Persson, and J. Harris, Phys. Rev. B **40**, 8146 (1989).
[5] At our impact conditions O_2 physisorbs on Cu(111) and desorbs reversibly when the target is heated resistively. Dissociation is apparently an unlikely process under these conditions. When adsorbed O_2 is desorbed by the laser pulses a low rate of dissociation is observed presumably due to an electronic excitation mechanism.
[6] H.-J. Ernst, F. Charra, and L. Douillard, Science **279**, 679 (1998).
[7] F. Althoff, T. Andersson, P. Linde, S. Andersson, and K. Burke (unpublished).
[8] Some of the peaks are narrow because of kinematical focusing for the condition $d\theta_s/d\epsilon_i = 0$ where θ_s is the scattering angle; see R. G. Rowe, L. Rathbun, and G. Ehrlich, Phys. Rev. Lett. **35**, 1104 (1975).
[9] G. Boato, P. Cantini, and L. Mattera, J. Chem. Phys. **65**, 544 (1976).
[10] W. Allison and B. Feuerbacher, Phys. Rev. Lett. **45**, 2040 (1981).
[11] G. Brusdeylins and J. P. Toennies, Surf. Sci. **126**, 647 (1983).
[12] K. Winkelmann, in *Rarefied Gas Dynamics*, Proceedings of the 11th International Symposium Vol. 11, edited by R. Camparque (Commisarat a l'Energie Atomique, Paris, 1979).
[13] F. Althoff, T. Andersson, and S. Andersson, Phys. Rev. Lett. **79**, 4429 (1997).
[14] J. Kimman, C. T. Rettner, D. J. Auerbach, J. A. Barker, and J. C. Tully, Phys. Rev. Lett. **57**, 2053 (1986).
[15] $V_0(z)$ varies only marginally between Cu(111) and C(100) [M. Persson and S. Andersson, Surf. Rev. Lett. **1**, 187 (1994)] and we have used parameters for D_2–Cu(100), as given in Ref. 19: $C_R = 5.21$ eV, $\alpha = 1.21 a_0^{-1}$, $C_{\mathrm{vdW}} = 4.74$ eV a_0^3, $z_{\mathrm{vdW}} = 0.563 a_0$, $k_c = 0.45 a_0^{-1}$.
[16] A. Chizmeshya and E. Zaremba, Surf. Sci. **268**, 432 (1992).
[17] J. Harris and P. J. Feibelman, Surf. Sci. **115**, L133 (1982); J. O. Hirschfelder, C. F. Curtiss, and R. B. Bird, *Molecular Theory of Gases and Liquids* (Wiley, New York, 1954).
[18] In practice, β_R was chosen so that $V(z,\theta)$ reproduces, at the classical turning point of the molecule, the anisotropy of a potential that was determined from total energy calculations, involving a lateral average over the top, bridge, and hollow sites. The calculations were performed with the plane-wave pseudopotential code DACAPO [DACAPO-1.30 of B. Hammer *et al.*, CAMP, DTH, Lyngby, Denmark], using the generalized gradient approximation for the exchange–correlation energy. The calculational unit cell contained a slab of four layers of Cu ions with three ions in each layer, resulting in a 4.47 Å separation between the molecules. The Cu slabs were separated by a vacuum layer that was five layers thick. The ion cores were represented by ultrasoft pseudopotentials, enabling a plane wave expansion cutoff at 30 Ry, and the surface Brillouin zone was sampled by 54 k points.
[19] L. Wilzén, F. Althoff, S. Andersson, and M. Persson, Phys. Rev. B **43**, 7003 (1991).
[20] J. C. Light, in *Time-Dependent Quantum Molecular Dynamics*, edited by J. Broeckhove and L. Lathouwers (Plenum, New York, 1992).
[21] G. G. Balint-Kurti and Á. Vibók, in *Numerical Grid Methods and Their Application to Schrödinger's Equation*, edited by C. Cerjan (Kluwer Academic, Dordrecht, 1993).
[22] In an extension of the work presented here, we plan to incorporate the effect of phonon losses in the calculations via a phenomenological optical potential.